

# Influence of substrate temperature on residual stress and nanomechanical properties of AlN films deposited by magnetron sputtering

Padmalochan Panda,<sup>1</sup> R. Ramaseshan,<sup>1, a)</sup> N. Ravi,<sup>2</sup> G. Mangamma,<sup>1</sup> Feby Jose,<sup>1</sup> S. Dash,<sup>1</sup> K. Suzuki,<sup>3</sup> and H. Suematsu<sup>3</sup>

<sup>1)</sup> *Surface and Nanoscience Division, Materials Science Group, Indira Gandhi Centre for Atomic Research, Kalpakkam 603102, India.*

<sup>2)</sup> *Center for Engineered Coatings, ARCI, Hyderabad 500005, India.*

<sup>3)</sup> *Extreme Energy Density Research Institute, Nagaoka University of Technology, Nagaoka, Japan.*

(Dated: 1 October 2018)

We report the crystal structure, surface morphology, residual stress and nanomechanical properties of Wurtzite type AlN thin films on Si (100) substrates using DC reactive magnetron sputtering with a function of substrate temperature (35 to 600 °C). Evolution of crystallite growth of AlN films was studied by GIXRD and transmission electron microscopy (TEM) and a preferred orientation of a-axis was observed at 400 °C. The cross-sectional TEM micrograph and selected area diffraction (SAD) pattern of AlN thin films showed that these films exhibited a high degree of orientation as well as the columnar structure. The surface morphology, roughness and grain size of these AlN films were investigated by atomic force microscopy (AFM) as a function of temperature. The residual stress of these films was calculated by  $\sin^2\psi$  technique and found that they are varying from tensile to compressive with temperature. Nanoindentation hardness ( $H$ ) of these films ranged between 12.8-19 GPa. We have observed an optimum deposition temperature of 400 °C for preferentially a-axis oriented AlN film with desired surface roughness and residual stress for surface acoustic wave devices (SAW).

PACS numbers: 81.15.-z; 81.15.Cd; 61.05.cp; 68.37.Ps; 68.37.Lp; 61.05.jm; 68.60.-p; 62.20.Qp

Keywords: Thin films, Sputtering, GIXRD, AFM, TEM, SAD, residual stress, hardness.

## I. INTRODUCTION

Aluminum nitride (AlN) is a versatile material with great technological advantages in semiconductor industry due to its wide band gap ( $\sim 6.2$  eV), high thermal conductivity (up to 320 W/mK) and small thermal-expansion coefficient.<sup>1-3</sup> It has been viewed as a highly promising material system for high-temperature (melting temperature  $\sim 3000$  °C) optoelectronic and short wavelength light source/detector applications.<sup>4-7</sup> AlN is a tetrahedrally coordinated III-V compound which crystallizes under ambient conditions in the thermodynamically stable hexagonal wurtzite structure.<sup>5</sup> It is used as optical films due to its high refractive index ( $\sim 2.0$  at a wavelength of 520 nm) as well as good dielectric constant ( $\sim 7$  at a frequency of 300 kHz).<sup>8</sup> Moreover, highly oriented AlN thin films deposited on silicon, have received considerable attention recently as an excellent piezoelectric material for surface acoustic wave devices on account of their high surface acoustic velocity as compared to ZnO, quartz and LiNbO<sub>3</sub>, etc.<sup>5,9-11</sup> Due to the similarity in crystal structure and lattice constant between AlN and GaN, the AlN film is also used as beneficial buffer layers for the growth of GaN films for optoelectronic devices.<sup>12</sup>

Highly efficient deep-ultraviolet light-emitting diode (UV-LED) is an expected future application where AlN

thin films find an important role with an emission wavelength of 210 nm (shortest wavelength ever observed from any semiconductor) using a p-i-n homojunction of a-plane oriented AlN. However, due to residual stress from the lattice mismatch and difference in thermal co-efficient of expansion between the substrate and thin film, its external quantum efficiency (EQE) is very low.<sup>13</sup> These have great influence on device performance not only in LED but also in high-power and high-frequency electronic devices. In the past decade, an extensive research work has been carried out on optimization of deposition by various coating techniques with deposition parameters in order to obtain the required reproducible quality thin film. Epitaxial growth of AlN has already been demonstrated on various monocrystalline substrates such as growth by chemical vapor deposition<sup>14</sup> on (0001) oriented AlN substrate at 1250 °C, molecular beam epitaxy<sup>15,16</sup> on GaN templates and Si (111) at 700 and 830 °C, respectively and deposition by pulsed laser deposition<sup>17</sup> on molybdenum at 450 °C. In most techniques, the deposition temperatures are quite high, so a smooth surface morphology of AlN films could not be obtained due to degradation of the substrate and thermal damage of AlN thin films during deposition.<sup>18</sup> Since large surface roughness may lead to increase in propagation loss especially when high frequency is reached. For SAW device applications using AlN thin films, a highly oriented film and homogeneous composition with low surface roughness is expected.<sup>19,20</sup> For that, reactive sputtering technique is a promising under such circumstances where, low sub-

<sup>a)</sup> seshan@igcar.gov.in

strate temperature deposition (wide variety of substrate materials, compatible with current semiconductor device processes) and good surface finish as well as adhesion are needed.<sup>21,22</sup> It is reported in the literature that AlN films deposited at low target to substrate distance (TSD) and low sputtering pressure exhibited (002) preferred orientation whereas those synthesized at high TSD and high pressure exhibited (100) orientation.<sup>23</sup> Medjani *et al.* reported the influence of substrate bias and explained a change from low to high resulted in the crystallographic orientation (002) to (100) at low TSD.<sup>24</sup> However, for applications, the fabrication of AlN thin film devices need a better understanding of the mechanical characterization in addition to its electrical and optical performances, since the contact loading during processing or packaging can significantly degrade the performance of these devices. So a precise measurement of the nano-mechanical characteristics of AlN films is required, where nanoindentation has been widely used to study the hardness, modulus and the deformation mechanisms.<sup>25,26</sup>

So, in this work, we have primarily concerned with the growth of AlN films at different substrate temperatures and have reported the evolution of orientation, residual stress, surface roughness and mechanical properties.

## II. EXPERIMENTAL

AlN thin films were synthesized by direct-current (DC) reactive magnetron sputtering technique, using MECA 2000 (France) from a water-cooled pure aluminum target (5N) of 50 mm diameter in a high purity argon (5N) and nitrogen (5N) gas mixture. P-type Si (100) substrates were cleaned by a standard two-step RCA process, boiled in a solution of H<sub>2</sub>O : NH<sub>4</sub>OH : H<sub>2</sub>O<sub>2</sub> (5:1:1). Then, they were etched in 2% HF-H<sub>2</sub>O solution for 2 min to remove the native oxide layers on the surfaces. Before deposition, the sputtering chamber was evacuated to  $1 \times 10^{-6}$  mbar by 1050 l/s turbo-molecular pump. First, in Ar atmosphere a very few Al mono layer was deposited on substrate for one minute to improve the adhesion between the substrate and to be deposited AlN thin film. The films were grown at different substrate temperatures at constant ratio of sputtering gas (Ar) to reactive gas (N<sub>2</sub>), target to substrate distance (TSD) and deposition pressure. The important deposition parameters in this study are listed in Table I. A surface profilometer (M/s. Dektak 6M, Veeco, USA) was used to measure the thickness of films and it was around 1  $\mu$ m.

Identification of crystalline phases was carried out by Grazing Incidence X-ray Diffraction (GIXRD) technique (M/s. Bruker D8, Germany) at a grazing angle of 0.5°. Cross section samples for transmission electron microscopy have been prepared in the conventional way using a focused ion beam apparatus (JIB-4500, JEOL, Japan). TEM investigations have been performed with an electron microscopy (M/s JEM-2100F, JEOL, Japan) operating at 200 kV. The SAD patterns were recorded

TABLE I. Deposition parameters of AlN films at different growth temperatures.

Sputtering parameters	Values
Target	Al (5N pure)
Substrate	Si (100)
Deposition pressure (mbar)	$3 \times 10^{-3}$
TSD (cm)	14
Ar : N <sub>2</sub> (sccm)	4 : 1
DC power (W)	200
Substrate temperature ( $T_s$ ) (°C)	35 to 600

using the same apparatus. The surface morphologies of these films were characterized by an atomic force microscope (NTEGRA Prima, M/s. NT-MDT, Russia) with a contact cantilever single-crystal silicon tip of size 10 nm. Bragg - Brantano (Cu -  $K_\alpha$ ) geometry was used to measure the residual stress of these films. The residual stress measurements of these films were carried out using  $\sin^2\psi$  technique with angle inclination ( $\psi$ ) varied from 0° to  $\pm 90^\circ$  with step size of 4°. An open platform nano indenter (M/s. HYSITRON, USA) equipped with a three sided pyramidal diamond berkovich tip was used to study the nanomechanical properties of these films at the peak load of 4000  $\mu$ N as followed by ISO14577 standard. Each experiments consist of 5 sec loading time, 2 sec hold time and 5 sec unloading time. The hardness ( $H$ ) and modulus ( $E$ ) value of these films were calculated following the Oliver and Pharr model.<sup>5</sup>

## III. RESULTS AND DISCUSSION

### A. GIXRD

The GIXRD profiles of AlN thin films sputtered on Si (100) with different substrate temperatures varying from 35 °C to 600 °C by DC magnetron sputtering are shown in Fig.1. The GIXRD patterns of these films show poly-crystalline hexagonal wurtzite structure and agree with the JCPDS data 25-1133. At 35 °C, it exhibited poly-crystalline nature, however with increase in substrate temperature from 100 to 500 °C, the crystallinity is increased as well as a preferred orientation has been observed. Particularly, at 100 and 400 °C substrate temperature, these films exhibited a preferential orientation towards a-axis, whereas 200 and 500 °C exhibited (101) orientation.

FWHM of AlN films which is decreasing with substrate temperature upto 400 °C is shown in Fig. 2. This phenomenon can be understood by the enhanced atom mobility at higher temperature, that increases the adatoms surface diffusion length, leading to a higher probability of adatoms migrate from the landing site to proper site. So that a better crystallinity and higher degree of preferred orientation is seen at 400 °C. However, further increasing the substrate temperature to 600 °C, FWHM

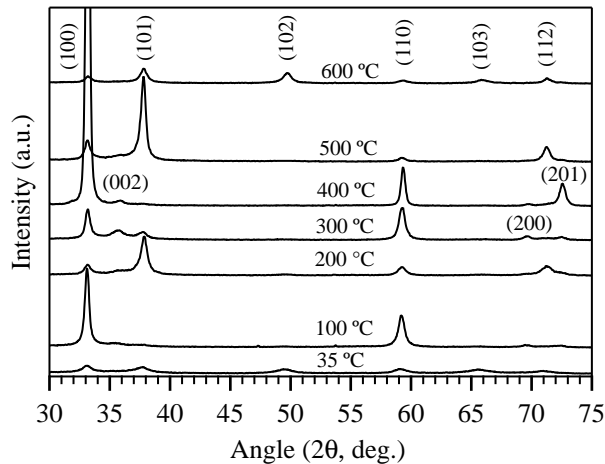


FIG. 1. GIXRD profiles of AlN thin films with different substrate temperatures.

as well as the intensity of other orientations are decreased. At higher temperatures, excessive surface mobility of adatoms make thin film unstable due to stronger re-evaporation effect which results in reducing the FWHM and intensity of the peaks.<sup>27</sup>

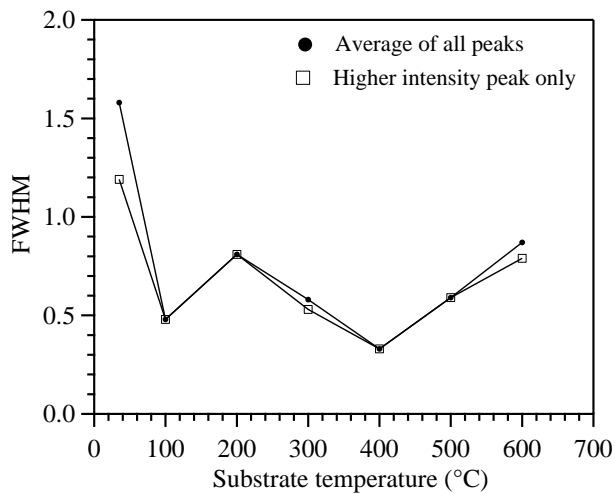


FIG. 2. The variation of FWHM of AlN thin films with different substrate temperatures.

Fig. 3 shows the crystallite lattice structure of AlN. In this wurtzite structure, each Al atom is linked by four N atoms forming a distorted tetrahedron with three Al-N<sub>(i)</sub> (i = 1, 2, 3) bonds, namely B<sub>1</sub>, the bond length is 0.1885 nm and one Al - N<sub>0</sub> in the c - axis direction, namely B<sub>2</sub>, the bond length is 0.1917 nm. The bond B<sub>2</sub> is more ionic character due to the coupling of Al empty orbit and the N full orbit, whereas B<sub>1</sub> is more covalent in nature due

to  $sp^3$  - hybridization between semi - full orbitals of Al and N atom.<sup>23,24</sup> The (100) plane is composed of the bonds B<sub>1</sub> which is more stronger as compared to B<sub>2</sub> bonds.

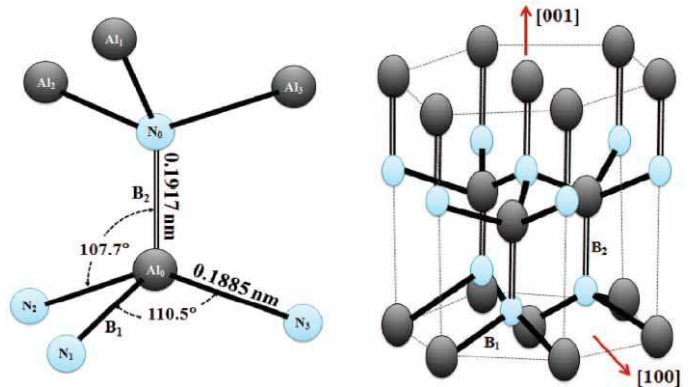


FIG. 3. (Color online) Crystal structure of wurtzite AlN.

So at high temperatures, B<sub>2</sub> bond can be easily dissociated which leads the increasing rate of vertical growth of the (100) planes. So, at 400 °C substrate temperature, the film is highly oriented along a-axis due to the (100) crystallites overgrowth the all other crystallites. But above 400 °C, different orientations are present, because this higher temperature is more favorable for the dissociation of both B<sub>1</sub> and B<sub>2</sub> bonds. Therefore, it can be concluded that the optimum substrate temperature for depositing highly a-axis oriented AlN films is 400 °C.

## B. TEM and SAED analyses

Figs. 4(a) and (b) show bright-field TEM cross sectional micrographs of AlN film grown on Si (100) substrate, deposited at 100 and 400 °C substrate temperature, respectively. The structure comprises parallel-spaced columnar structure with slightly deviating by a few degrees from the substrate normal due to magnetron gun inclination with respect to the substrate where the contrast is from the grains. So the sputtered atom flux is arriving obliquely at an angle  $\alpha$  and causes the inclination of the columns by  $\beta$  where  $\alpha$  and  $\beta$  are related by the empirical tangent-rule :  $\tan \beta = 1/2 \tan \alpha$ .<sup>28</sup> The interface is fairly flat and an amorphous-like layer of few nm thick is revealed at the AlN film/Si interface of the film grown at 100 °C. However, the film grown at 400 °C, shows a very thin amorphous-like layer at the interface as compared to 100 °C film. This interface roughening are possible due to initial surface oxide intermixing between silicon and AlN as well as strong lattice mismatch.<sup>2,29</sup> So the evolution of amorphous structure at the interface of AlN film/Si reveals that the higher the growth temperature, the better the crystallinity as well as with columnar structure.

Figs. 4(c) and (d) shows the corresponding selected area diffraction (SAD) pattern of these film deposited

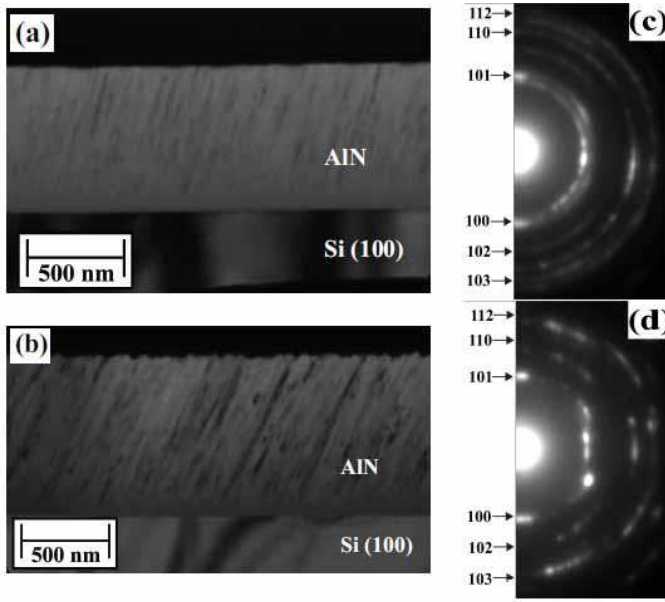


FIG. 4. The bright-field cross-sectional TEM image of AlN film deposited on Si at (a) 100 °C, (b) 400 °C substrate temperatures and SAD pattern of AlN film deposited at (c) 100 °C, (d) 400 °C substrate temperatures, respectively.

at 100 and 400 °C substrate temperature, respectively. All the diffraction rings are brighter and could be indexed from crystalline AlN, space group  $P6_3mc$ , lattice constants  $a=0.311$  nm and  $c=0.497$  nm (JCPDS file 25-1133). The diffracted ring pattern with the reflection spots was observed which shows the good textural growth of the film. The deposited film showed a polycrystalline microstructure with the mixed planes of AlN (100), (101), (102), (110), (103) and (112). These patterns shows that at 400 °C substrate temperature, AlN films is well crystallized with highly oriented along a-axis than that of deposited at 100 °C substrate temperature.

### C. Morphology and surface roughness investigated by AFM of AlN films

Due to excellent piezoelectric response, AlN films are used in SAW devices. So its microstructure and surface roughness have a crucial character on the performance of these devices. Surface acoustic wave cannot pass through the surface of a material if the surface roughness is greater than the wavelength.<sup>19,20</sup> Fig. 5 consists of AFM images over  $1.5 \times 1.5 \mu m$  surface area showing the morphology of the AlN films deposited on Si (100) substrate at various substrate temperatures. In Fig. 5 (a,b), AlN deposited at 35 and 100 °C exhibits irregular grains with less dense surface. But with the increase in substrate temperature from 200 °C to 600 °C, a similar morphology can be seen and having a pebble-like grain structure with dense surface.

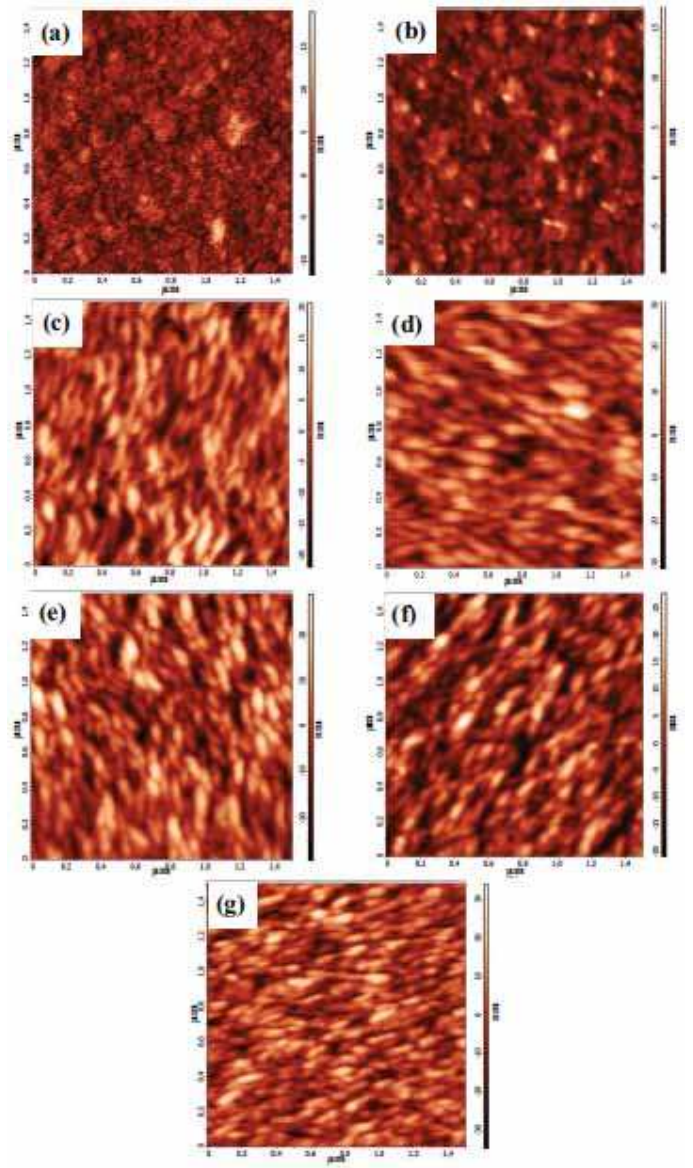


FIG. 5. (Color online) AFM images of AlN films on Si (100) with growth temperatures (a) 35 °C, (b) 100 °C, (c) 200 °C, (d) 300 °C, (e) 400 °C, (f) 500 °C, and (g) 600 °C.

The micrographs show that AlN films exhibit fine grains and dense structure with increasing substrate temperature. Fig. 6 displays the root mean square (RMS) surface roughness and the mean diameter of grains of the films with increase in temperature. RMS roughness and average grain size are significantly affected by the increase in substrate temperature. Because of thermal energy delivered to the surface that enhances the energy and mobility of surface adatoms as well as atomic diffusion. This resulted in the formation of fewer large grains by agglomeration of adjoining atoms or crystals and make surface coarser with the substrate temperature. This can be seen from the cross-sectional TEM image (Fig. 4), the

waviness is pronounced more in 400 °C substrate temperature. But, after 500 °C, roughness is decreasing due to decrease in grain size and crystallinity which can be seen from the FWHM of these films in Fig 2. Generally, the surface roughness of the films is required to be less than 30 nm. From this point of view, this surface roughness is very suitable for surface acoustic wave and bulk acoustic wave devices.

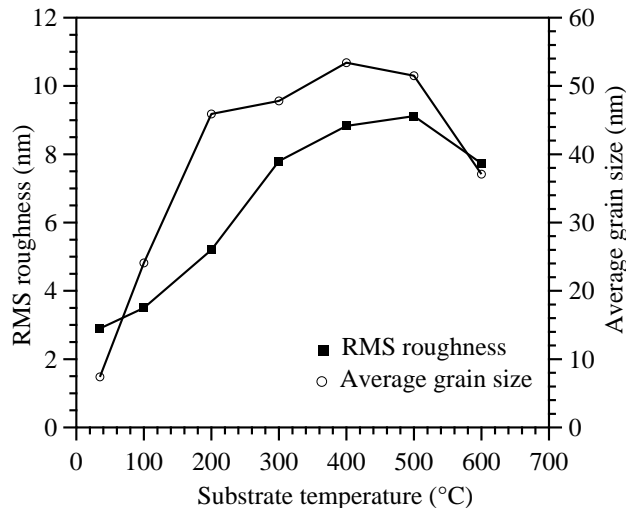


FIG. 6. The surface roughness RMS values and average grain sizes measured from the AFM images versus the substrate temperatures of AlN films.

#### D. Residual stress analysis of AlN films

Residual stress plays an important role on thin films since it alters the physical properties like energy-band structure, external quantum efficiency of LED, mechanical properties. This may cause micro-cracks or peeling from the substrate as well as the poor performance and lifetime of the coated component. Therefore, it is important to control the residual stress by controlling the sputtering parameters to synthesize a mechanically stable AlN films.

Measurement of residual stresses (in-plane stresses) has been carried out by a well-documented  $\sin^2\psi$  technique where crystallographic planes tilted at multiple angles ( $\psi$ ), from the surface normal.<sup>30</sup> There is a correlation between the stress components in the film and variation in d-spacing with tilt angle ( $\psi$ ). The slope of the linear relationship between d-spacing and  $\sin^2\psi$  is proportional to the stress component operative in the plane of the specimen along the direction of the diffraction vector according to the equation shown below

$$\frac{(d_\psi - d_0)}{d_0} = \left[ \left( \frac{1 + \nu}{E} \right)_{(hkl)} \sigma_\varphi \sin^2\psi \right] - \left[ \left( \frac{\nu}{E} \right)_{(hkl)} (\sigma_1 + \sigma_2) \right] \quad (1)$$

where E - Young's modulus,  $\nu$  - Poisson's ratio,  $\left( \frac{d_\psi - d_0}{d_0} \right)$  - micro-strain,  $\left( \frac{1 + \nu}{E} \right)$ ,  $\left( \frac{-\nu}{E} \right)$  are X-ray elastic constants and  $\sigma_1, \sigma_2$  are principal stresses. For all practical purposes, the Equation (1) can be reduced to:

$$d_\psi = \left[ \left( \frac{1 + \nu}{E} \right)_{(hkl)} d_0 \sigma_\varphi \sin^2\psi \right] + d_0 \quad (2)$$

The observed residual stress of all these films are plotted as a function of substrate temperature shown in Fig. 7. A tendency from tensile to compression is observed with increase in substrate temperature. The residual stress has decreased from 0.42 GPa to 0.27 GPa when the substrate temperature increased from 35 °C to 300 °C (tensile stress). However, for the substrate temperature 400 °C to 600 °C, the residual stress has changed from -0.14 GPa to -0.15 GPa (compressive stress).

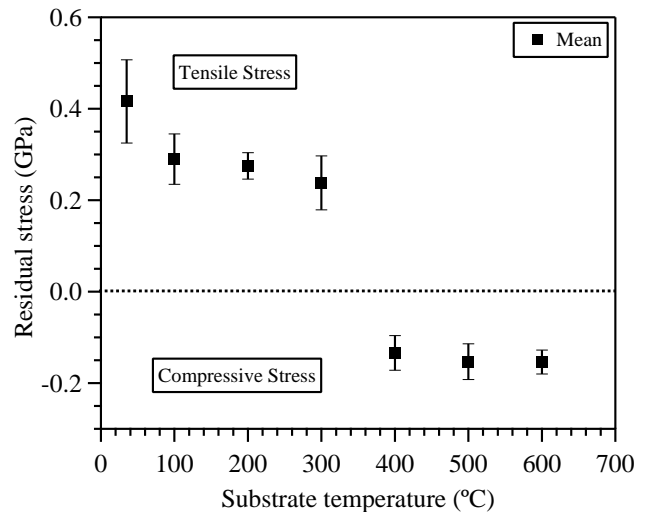


FIG. 7. Residual stress of AlN thin films as a function of substrate temperatures.

In general, the origin of residual stress can be attributed to the epitaxial stress (lattice mismatch between substrate and the film), thermal stress (difference in thermal co-efficient of expansion between substrate and the film), microstructure and the mode of growth. The thermal expansion coefficient of AlN film is larger than that of the Si substrate that developed a compressive stress as the sample is cooled down to room temperature from a high temperature since the film thickness is very negligible as compared to the substrate thickness. This thermal stress can be calculated using the relation<sup>31</sup>

$$\sigma_T = \frac{E_f}{(1 - \nu_f)}(\alpha_s - \alpha_f)(T_s - T_r) \quad (3)$$

where  $\sigma_T$  is thermal stress,  $\alpha_s$  and  $\alpha_f$  are thermal expansion coefficients of the substrate (Si,  $3.6 \times 10^{-6} C^{-1}$ ) and the film (AlN,  $5.3$  and  $4.2 \times 10^{-6} C^{-1}$  along a-axis and c- axis, respectively),  $T_r$  and  $T_s$  are room and substrate temperature,  $E_f$  and  $\nu_f$  are the Young's modulus (AlN, 350 GPa) and the Poisson's ratio of film (AlN, 0.21).<sup>32,33</sup> Substituting the respective values and substrate temperature the thermal stress has been calculated which is shown in Table II.

TABLE II. Thermal stress of a-axis and c-axis AlN films at different substrate temperatures.

$T_s$ (°C)	$\sigma_T$ (a-axis) (GPa)	$\sigma_T$ (c-axis) (GPa)
35	-0.007	-0.002
100	-0.056	-0.019
200	-0.131	-0.046
300	-0.207	-0.073
400	-0.282	-0.099
500	-0.357	-0.126
600	-0.433	-0.152

Intrinsic or growth stress is a structure and microstructure sensitive property which is observed in films during deposition or growth under non-equilibrium conditions. In the early stages of film growth, the film consists of smaller crystallites/grains, separated by an atomic-scale distance. When these crystallites/grains coalesce, a tensile stress is generated at the point where neighboring islands impinge on each other.<sup>34</sup> As well as, the parameter  $T_s/T_m$  ( $T_s$  = substrate temperature and  $T_m$  = melting temperature of coating material) is very important in stress-related behavior for different materials. For higher melting point materials, the parameter  $T_s/T_m$  is typically low during deposition. So, under these conditions intrinsic stress can dominate over thermal stress.<sup>35</sup> Because, when these AlN films deposited at room temperature, there is a little surface diffusion and one would expect the Al or N vacancy concentration to be much larger than at equilibrium. When these excess vacancies are subsequently annihilated at vertical boundary, the associated volume change results in an in-plane change of film dimensions.<sup>36</sup> So at lower growth temperatures, stress relaxation by diffusion does not occur where intrinsic stress dominates over the thermal stress and a tensile stress develops. But with increase in substrate temperature, the diffusion of defects and vacancies in AlN lattice microstructure causes the decrease in residual stress due to film densification by decreasing the void regions through enhanced atomic rearrangement. Above 400 °C, the thermal stress is dominating. So the residual stress changes from tensile to compressive stress.

It can be reasoned in Fig. 7 that substrate temperature plays a major role on residual stress of sputtered AlN

films. a-axis orientated AlN film shows a compressive stress at 400 °C substrate temperature. Moreover compressive residual stress is usually expected to improve the quality of the cutting tools and engine cylinder coatings.

## E. Nanomechanical properties

Mechanical characterization is essential to understand and solve the problem of controlling residual stress/strain and defect density in the film for design of devices. Nanoindentation studies were performed to estimate the mechanical properties of the films at the peak load of 4000  $\mu$ N. The absence of creep and thermal drift was verified by holding the indenter at maximum load for 2 sec (no change in penetration depth). Initially, the hardness ( $H$ ) increased steadily with substrate temperature until it reached 200 °C, where a maximum  $H$  of 19 GPa was observed (Fig. 8). Then, further increase in substrate temperature led only to a constant drop in hardness, down to 12.8 GPa for a substrate temperature 600 °C. In general, orientation of the film, crystallite

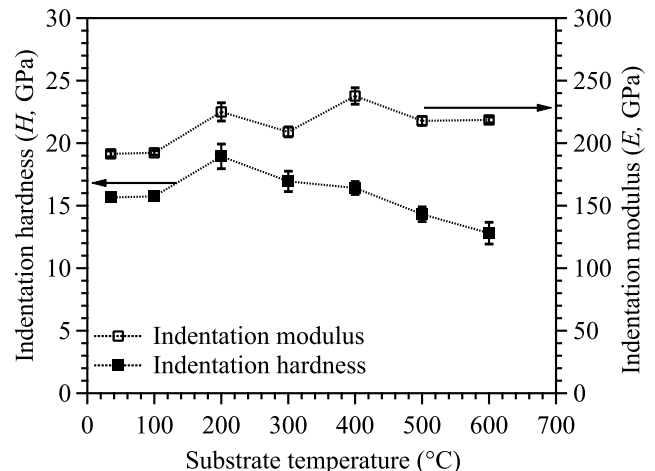


FIG. 8. Variation in hardness and modulus against substrate temperature.

size and residual stress collectively contributes to the improvement of mechanical properties of the films.<sup>37</sup> Recalling the evolution of the growth structure (TEM (Fig.4) and AFM (Fig.5)) stress relaxation in larger crystallites formed at higher substrate temperature that can be seen from FWHM, average grain size and residual stress of these films in Fig. 2, 6 and 7, respectively. On the other hand, nanoindentation modulus ( $E$ ) of these AlN films is also varied from 191.5 to 237.6 GPa with different substrate temperature. Generally, modulus depends on the nature of inter-atomic bonds in the crystal. At 400 °C substrate temperature, AlN film is highly a-axis oriented which contains  $B_1$  type of bonds (more covalent). So this

film is showing high elastic nature where the indentation modulus is 237.6 GPa.

However, it is possible to produce films with the same  $H$  and different values of  $E$  i.e. films with the same hardness can exhibit different resistance to plastic deformation. For a protective film such as AlN, it is important to understand whether hardness value is giving true resistance to plastic deformation during contact event. For that the ratio of  $H^3/E^2$  has been widely applied to evaluate the resistance to plastic deformation from the value of  $H$  and  $E$ .<sup>38</sup> Fig. 9 shows the value of  $H^3/E^2$  of AlN films as a function of substrate temperature. So the parameter  $H^3/E^2$  is also following same profile as the hardness with increase in substrate temperature. It is also evident from the inset of Fig. 9 that there is an approximately linear relationship, in  $H^3/E^2$  with the range of hardness of these films which agrees with Beake and co-workers general correlation between  $H^3/E^2$  and  $H$ .<sup>38</sup>

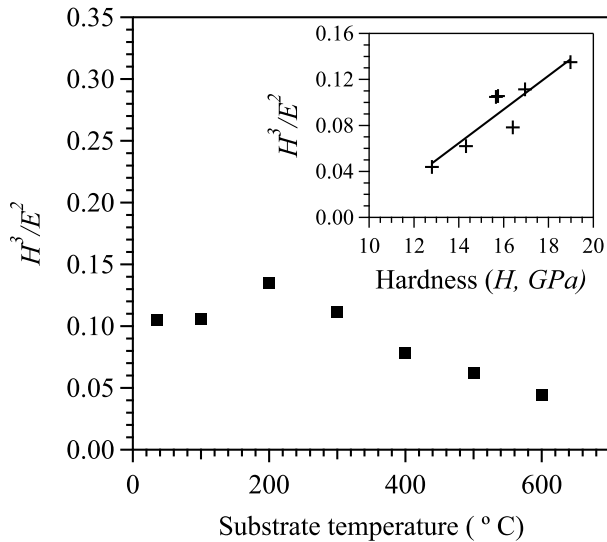


FIG. 9. Variation in  $H^3/E^2$  against substrate temperature of AlN films. The  $H^3/E^2$  is plotted against indentation hardness in the inset.

#### IV. CONCLUSION

DC reactive magnetron sputtering has been used to synthesize AlN thin films on Si (100) substrate at different substrate temperatures varying from 35 to 600 °C. We have observed all the films crystallized with wurtzite structure and the substrate temperature influenced the orientation of the AlN films. The crystallinity increased with temperature and preferred orientation (a-axis) was observed at 400 °C. The cross section and SAD pattern of AlN films by TEM investigation showed a high degree of alignment (columnar structure) as well as the orientation. The surface morphology, RMS roughness

and average grain size are also strongly influenced by the substrate temperature. However the residual stress measurement by  $\sin^2\psi$  technique showed tensile stress up to 300 °C and then changed to compressive stress from 400 °C to 600 °C. Nano-indentation hardness studies on these films revealed that the indentation hardness ( $H$ ) varied between 19 to 12.8 GPa where as at 400 °C substrate temperature AlN film is showing high elastic nature ( $E = 237.6$  GPa). The optimum condition for the growth of a-axis orientated AlN film is at sputtering power of 200 W, pressure of  $3 \times 10^{-3}$  mbar, Ar : N<sub>2</sub> at 4 : 1 sccm, TSD of 14 cm and deposition temperature 400 °C, giving a good compromise between surface morphology, RMS roughness, residual stress and nanomechanical properties for SAW devices.

#### V. ACKNOWLEDGMENTS

The authors would like to thank UGC-DAE Consortium for Scientific Research, Kalpakkam, India for giving the facility of GIXRD.

#### REFERENCES

- <sup>1</sup>Hadis Morkoc, Handbook of Nitride Semiconductors and Devices. Vol.1 : Materials Properties, Physics and Growth (WILEY-VCH, Weinheim, 2008) p. 23-29.
- <sup>2</sup>T. S. Pan, Y. Zhang, J. Huang, B. Zeng, D. H. Hong, S. L. Wang, H. Z. Zeng, M. Gao, W. Huang, and Y. Lin, J. Appl. Phys. 112 (2012) 044905.
- <sup>3</sup>Safa Kasap, Peter Capper (Eds.), Handbook of Electronic and Photonic Materials (Springer, NewYork, 2006) p. 753-795.
- <sup>4</sup>F Litimein, B Bouhaf, Z Dridi and P Ruterana, New Journal of Physics 4 (2002) 64.1-64.12.
- <sup>5</sup>Feby Jose, R. Ramaseshan, S. Tripura Sundari, S. Dash, A. K. Tyagi, M. S. R. N. Kiran, and U. Ramamurty, Appl. Phys. Lett. 101 (2012) 254102.
- <sup>6</sup>A. Soltani, A. Stolz, J. Charrier, M. Mattalah, J. C. Gerbedoen, H. A. Barkad, V. Mortet, M. Rousseau, N. Bourzgui, A. Ben-Moussa, and J. C. De Jaeger, J. Appl. Phys. 115 (2014) 163515.
- <sup>7</sup>H. A. Barkad, A. Soltani, M. Mattalah, J.-C. Gerbedoen, M. Rousseau, J.-C. De Jaeger, A. BenMoussa, V. Mortet, K. Haenen, B. Benbakhti, M. Moreau, R. Dupuis, and A. Ougazzaden, J. Phys. D: Appl. Phys. 43 (2010) 465104.
- <sup>8</sup>V. Dimitrova, D. Manova, E. Valcheva, Materials Science and Engineering, B68 (1999) 1-4.
- <sup>9</sup>M. Clement, L. Vergara, J. Sangrador, E. Iborra, A. Sanz-Hervas, Ultrasonics 42 (2004) 403407.
- <sup>10</sup>Thierry Aubert, Jochen Bardong, Ouarda Legrani, Omar Elmazria, M. Badreddine Assouar, Gudrun Bruckner and Abdelkrim Talbi, J. Appl. Phys. 114 (2013) 014505.
- <sup>11</sup>Sean Wu, Ruyen Ro, Zhi-Xun Lin, and Maw-Shung Lee, J. Appl. Phys. 104 (2008) 064919.
- <sup>12</sup>Matt D. Brubaker, Igor Levin, Albert V. Davydov, Devin M. Rourke, Norman A. Sanford, Victor M. Bright, and Kris A. Bertness, J. Appl. Phys. 110 (2011) 053506.
- <sup>13</sup>Shibo Yang, Reina Miyagawa, Hideto Miyake, Kazumasa Hiramatsu and Hiroshi Harima, Appl. Phys. Exp. 4 (2011) 031001.
- <sup>14</sup>I. Bryan, A. Rice, L. Hussey, Z. Bryan, M. Bobea, S. Mita, J. Xie, R. Kirste, R. Collazo, and Z. Sitar, Appl. Phys. Lett. 102 (2013) 061602.

- <sup>15</sup>Yonghui Wu, C.H. Jia, W.F. Zhang, *Diamond and Related Materials* 25 (2012) 139-143.
- <sup>16</sup>T. Kuyoma, M. Sugawara, Y. Uchiyama, J. F. Kaeding, R. Sharma, T. Onuma, S. Nakamura, and S. F. Chichibu, *Phys. Status Solidi A* 203 (2006) 1603-1606.
- <sup>17</sup>K. Okamoto, S. Inoue, T. Nakano, T.-W.Kim, M. Oshima, and H. Fujioka, *Thin Solid Films* 516 (2008) 4809-4812.
- <sup>18</sup>H.Y. Liu, G.S. Tang, F. Zeng, F. Pan, *Journal of Crystal Growth* 363 (2013) 80-85.
- <sup>19</sup>Duy-Thach Phan, Gwi-Yang Chung, *Applied Surface Science* 257 (2011) 8696-8701.
- <sup>20</sup>Xu-Ping Kuang, Hua-Yu Zhang, Gui-Gen Wang, Lin Cui, Can Zhu, Lei Jin, Rui Sun, Jie-Cai Han, *Superlattices and Microstructures* 52 (2012) 931-940.
- <sup>21</sup>F. Engelmark, G. Fucntes, I. V. Katardjiev, A. Harsta, U. Smith, and S. Berg, *J. Vac. Sci. Technol. A* 18 (2000) 1609-1612.
- <sup>22</sup>C. Mirpuri, S. Xu, J. D. Long, and K. Ostrikov, *J. Appl. Phys.* 101 (2007) 024312.
- <sup>23</sup>X.H. Xu, H.S. Wu, C.J. Zhang, Z.H. Jin, *Thin Solid Films* 388 (2001) 62.
- <sup>24</sup>F. Medjani, R. Sanjines, G. Allidi and A. Karimi, *Thin Solid Films* 515 (2006) 260-265.
- <sup>25</sup>Martin T. K. Soh, A. C. Fischer-Cripps, N. Savvides, C. A. Musca and L. Faraone, *J. Appl. Phys.* 100 (2006) 024310.
- <sup>26</sup>Feby Jose, R. Ramaseshan, S. Dash, S. Bera, A. K. Tyagi, and Baldev Raj, *J. Phys. D: Appl. Phys.* 43 (2010) 075304.
- <sup>27</sup>Kuan-Hsun Chiu, Jiann-Heng Chen, Hong-Ren Chen, Ruey-Shing Huang, *Thin Solid Films* 515 (2007) 4819-4825.
- <sup>28</sup>S. Mahieu, P. Ghekiere, D. Depla, R. De Gryse, *Thin Solid Films* 515 (2006) 1229-1249.
- <sup>29</sup>J.X. Zhang, Y.Z. Chen, H. Cheng, A. Uddin, Shu Yuan, K. Pita, T.G. Andersson, *Thin Solid Films* 471 (2005) 336-341.
- <sup>30</sup>ShyamalRao Polaki, Rajagopalan Ramaseshan, Feby Jose, S. Dash, A. K. Tyagi, Nukala Ravi, *Int. J. Appl. Ceram. Technol.* 10 (2013) 45-50.
- <sup>31</sup>Chuen-Lin Tien, Tsai-Wei Lin, Kuo-Chang Yu, Tsung-Yo Tsai and Hsi-Fu Shih, *IEEE TRANSACTIONS ON MAGNETICS*, 50(7) (2014) 2005304.
- <sup>32</sup>W. M. Yim and R. J. Paff, *J. Appl. Phys.* 45 (1974) 1456.
- <sup>33</sup>Bernd Hhnlein, Peter Schaaf, and Jrg Pezoldt, *J. Appl. Phys.* 116 (2014) 124306.
- <sup>34</sup>Brian W. Sheldon, K. H. A. Lau, and Ashok Rajamani, *J. Appl. Phys.* 90 (2001) 5097-5013.
- <sup>35</sup>John A. Thornton and D. W. Hoffman, *Thin Solid Films*, 171 (1989) 5-31.
- <sup>36</sup>J.Y. Song, Jin Yu, *Thin Solid Films* 415 (2002) 167-172.
- <sup>37</sup>P.H.Mayrhofer, F.Kunc , J.Musil , C.Mitterer, *Thin Solid Films* 415 (2002) 151-159.
- <sup>38</sup>B D Beake, V M Vishnyakov, R Valizadeh and J S Colligon, *J. Phys. D: Appl. Phys.* 39 (2006) 1392-1397.